Excitonic luminescence of the Br_2-intercalated layered semiconductors $2H$-WS_2

L. Kulyuk and D. Dumcehnko
Institute of Applied Physics, Academy of Sciences of Moldova, Academiei str. 5, Chisinau, MD-2028, Republic of Moldova

E. Bucher, K. Friemelt, and O. Schenker
Department of Physics, University of Konstanz, P.O. Box X916, D-78457 Konstanz, Germany

L. Charron, E. Fortin, and T. Dumouchel
Department of Physics, University of Ottawa, Ontario K1N6N5, Canada
(Received 16 March 2005; published 15 August 2005)

Radiative recombination processes in the transition metal dichalcogenide compound $2H$-WS_2 are investigated. The strong sharp line photoluminescence in the spectral range 1.32–1.34 eV is attributed to the recombination of excitons bound on electron-attractive neutral centers, formed by Br_2 molecules intercalated in the van der Waals gap of the $2H$-WS_2 layered crystals. These centers, located at energy E_T=0.1 eV below the conduction band, display properties similar to the acceptorlike isoelectronic traps in GaP or Si, providing efficient radiative recombination. The temperature dependence of the zero-phonon spectral line intensities and of the luminescence decay time is described in the framework of a kinetic model in thermal equilibrium conditions. The atypical temperature increase of the luminescence decay time in the temperature range T =2–7 K is related to the presence of a long lifetime sublevel, situated at 0.3 meV above the lowest excitonic state. The observed broadband emission centered at 0.97 eV is ascribed to recombination via a deep center due to an instrinsic defect of the layered crystal.

DOI: 10.1103/PhysRevB.72.075336 PACS number(s): 78.55.Hx, 71.35.Gg, 78.55.−m

I. INTRODUCTION

The hexagonal $2H$-polytype of tungsten disulphide WS_2 belongs to the class of transition metal dichalcogenides that exhibit many physical properties with a pronounced two-dimensional character.[1,2] The peculiar properties of these materials result from their layered structure ($P6_3/mmc-D^4_{6h}$), consisting of covalently bonded S-W-S sheets linked by weak van der Waals forces. Within each sheet there is a trigonal prismatic coordination between the metal and chalcogenide atoms. Like the other transition metal dichalcogenide compounds, WS_2 is an indirect-gap semiconductor with the valence band maximum located at the center of the Brillouin zone and the conduction minimum between Γ and K points.[1,3–6] The energy of the indirect band gap is E_g =1.35 eV at room temperature[6–8] and 1.45 eV at T=80 K.[9] The smallest direct optical transition associated with excitonic absorption peak at energy of 2.05 eV (77 K)[1,3,10,11] is located at the K point of the Brillouin zone.[3–5]

Owing to the layered structure, the electronic properties of the transition metal dichalcogenides can be essentially modified by intercalation of different chemical species between layers.[12] The iodine, bromine, or chlorine usually used as transport agents for crystal growth by halogen vapor transport[13] can also be treated as intercalants. The influence of the interlayer halogen impurities, incorporated during the crystal growth, on the electrical properties of the $MoTe_2$ single crystals were revealed in Ref. 14. However, subsequently, in spite of numerous papers on intercalation complexes of transition metal dichalcogenides,[12,15,16] as well as of a direct analogy with bromine intercalated graphite compounds,[17] the intercalation of halogen molecules in lamellar TX_2 crystals has been not investigated.

Recently we reported an observation of the excitonic luminescence in tungsten dichalcogenides layered compounds $2H$-WS_2 and $2H$-WSe_2, intercalated by Br_2 and I_2 molecules during the crystal growth processes.[18] The halogen molecule placed in the adjacent tetrahedral sites of the gap gives rise to the neutral radiative center, with properties, similar to that of the isoelectronic impurities in GaP (Ref. 19) or Si,[20] which provide the strong bound-exciton luminescence of the indirect band gap semiconductor. Excitonic photoluminescence (PL) has been also observed in synthetic $2H$-MoS_2 single crystals grown using chlorine Cl_2 as the transport agent.[21] It was shown that the PL spectral lines at energies near 1.2 eV have an origin similar to that of the excitonic emission in tungsten dichalcogenides, that is the recombination of excitons bound to the centers formed by the halogen (Cl_2) molecules. For natural MoS_2 samples (mineral molybdenite, grown without any transport agents) excitonic luminescence was not observed. However, as in the case of the synthetic MoS_2 crystals containing chlorine, a broadband IR emission centered at 0.95 eV was detected. This vibronic emission band has been associated with an intrinsic defect of the MoS_2 crystalline lattice, inherent to both types of samples.

Thus, the intercalation of transition metals dichalcogenides by halogen molecules provides a potential use of these layered materials: Now, besides applications in such important areas as photovoltaic solar cells,[22] solid lubricants,[23] or intercalation batteries[11,16] (and references therein), the TX_2 compounds could be of interest as efficient luminescent materials in the near IR spectral region. It is appropriate to mention that recently synthesized MoS_2 nanotube bundles contained iodine;[24] iodine was used as a transport agent and plays a crucial role in the formation of the structure of these low-dimensional dichalcogenide systems.[25]

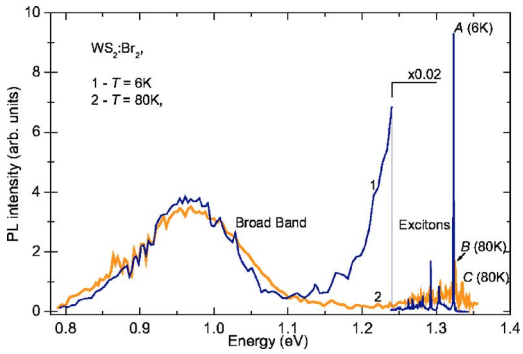

FIG. 1. (Color online) Photoluminescence spectra of $2H$-WS_2:Br_2 layered crystals at 6 and 80 K.

In this paper the results of systematic investigations of the excitonic luminescence of Br_2 intercalated $2H$-WS_2 single crystals are presented. The observed temperature evolution of the steady-state emission spectra, the fast thermal quenching, as well as the temperature dependence of the luminescence decay time are described in the framework of a kinetic model applied to a *n*-type compensated semiconductor in thermal equilibrium conditions.

II. EXPERIMENTAL RESULTS

The $2H$-WS_2 single crystals were grown at University of Konstanz (Konstanz, Germany) by means of chemical vapor transport using bromine as transport agent.[10,13] The presence of a small amount of bromine ($\sim 2\times 10^{-1}$ at. % in the $2H$-WS_2 samples) was determined by x-ray microanalysis on a "Siemens" sequential x-ray spectrometer SRS-3000. The electron concentration as measured by standard Hall effect technique was $n_o \approx 10^{15}$–10^{16} cm^{-3} at room temperature and about 10^{10}–10^{11} cm^{-3} at $T<140$ K. The samples investigated were a few millimeters in diameter and a few tens of micrometers thick.

The photoluminescence (PL) measurements in the temperature range $T=2$–120 K were performed with a variable-temperature optical cryostat, a one-meter grating Czerny-Turner monochromator coupled to a liquid nitrogen cooled Ge detector or a photomultiplier with a $S1$ photocathode, using either standard lock-in detection techniques or a digitizing scope. The steady-state luminescence was excited using a Kr-ion laser (568 nm line) or a diode-pumped cw solid-state laser (532 nm). The time resolved PL was excited by the 532 nm (2.34 eV) output from a frequency doubled Q-switched YAG:Nd pulsed laser ($\Delta\tau \approx 10^{-8}$ s).

The PL spectra of $2H$-WS_2:Br_2, as in the case of synthetic $2H$-MoS_2:Cl_2,[21] consist of two parts (Fig. 1): a short-wave excitonic region ($E_{exc} \approx 1.25$–1.34 eV), which includes several sharp intense lines, and a relatively weak broadband centered at 0.97 eV with a half-width of about 0.15 eV.

Figure 2 shows the temperature evolution of the excitonic emission spectrum. At low temperatures the spectra are dominated by two narrow lines A and B, separated by $\Delta_{AB}=3.0$ meV. The energies of the doublet peaks $E_A=1.323$ eV, $E_B=1.326$ eV, are smaller by approximately 0.12 eV than the indirect band gap energy of the WS_2. Figure 3 shows the

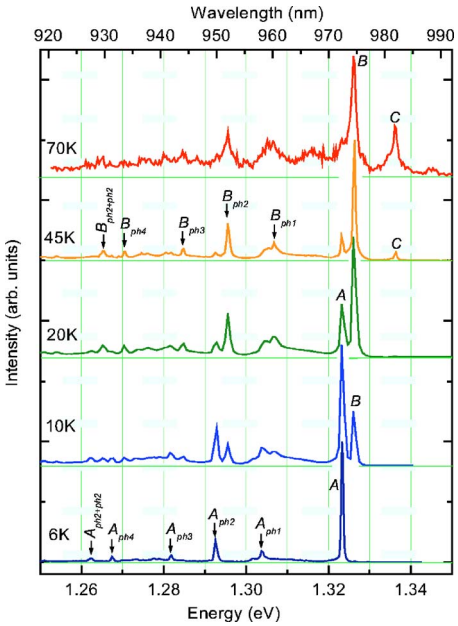

FIG. 2. (Color online) Bound-exciton emission spectra of $2H$-WS_2:Br_2 at different temperatures. The phonon replicas of the A and B electronic lines labeled A_{ph1}-A_{ph4} and B_{ph1}-B_{ph4} are shown at 6 and 45 K. Peaks marked $A_{ph2+ph2}$ and $B_{ph2+ph2}$ are $2E_{ph2}$ replicas of the respective no-phonon lines.

intensities of the two lines and the integral intensity of the doublet versus $1000/T$ in a semi-logarithmic plot. When the temperature increases, the PL intensity is redistributed from the long wavelength peak A to peak B, while the integral intensity of the doublet does not depend on T and remains constant up to 50 K. Such a temperature evolution confirms that the observed lines originate from a unique radiative center. The contribution of the third line C ($E_C=1.336$ eV, $E_C-E_A=13$ meV), which can be observed beginning from $T>20$ K, is quite small. At $T>70$ K the amplitude of line C becomes comparable to that of line B; however, above 50 K a fast thermal quenching of the excitonic emission occurs (Fig. 3). The thermal activation energy of this exponential quenching is 0.1 eV. The broadband emission intensity re-

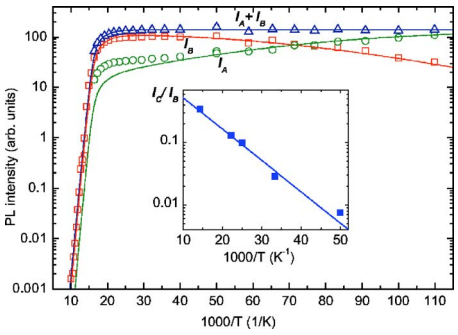

FIG. 3. (Color online) Temperature dependence of the A-B doublet intensities: The open squares and circles are experimental points; the open triangles represent the sum of the A and B peak intensities; the solid lines are theoretical fits according to Eqs. (7). Shown in the inset is the ratio of the C- and B-line intensities as a function of $1000/T$ [solid line–calculated ratio $\eta_4^{(C)}(T)/\eta_3^{(B)}(T)$].

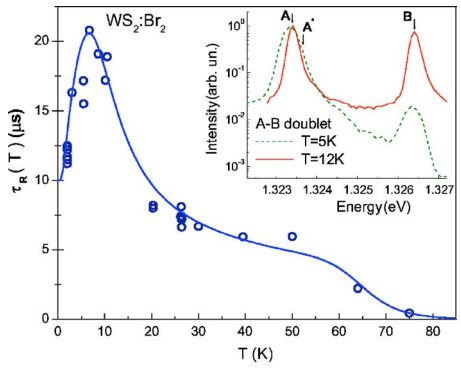

FIG. 4. (Color online) Temperature dependence of the PL decay time. The curve represents the fit of Eq. (1) to the experimental data (circles). In the inset—the *A*-*B* excitonic doublet at low temperatures (in order to detect the *B* peak, the spectrum at 5 K was taken at lower resolution).

mains practically constant in the whole temperature range where excitonic luminescence is observed (Fig. 1). As in $2H$-MoS_2 (Ref. 21) thermal quenching of the IR broadband emission starts at $T>100$ K.

The main phonon replicas of the A,B, and C lines are shifted by $E_{ph1}=19.5$ meV (157 cm^{-1}), $E_{ph2}=30.7$ meV (247 cm^{-1}), $E_{ph3}=41.6$ meV (335 cm^{-1}), and $E_{ph4}=55.9$ meV (450.8 cm^{-1}) to the Stokes side of the spectrum (Fig. 2). These shifts, being quite different from the frequencies of the infrared- and Raman-active modes in $2H$-WS_2 crystals,[6,26–28] can be ascribed to the local vibronic modes of the impurity center, which provides the radiative recombination.

Figure 4 (circles) shows the experimental temperature dependence of the luminescence decay time of the zero phonon lines. The temporal decay was exponential at all temperatures (2–70 K). The initial temperature increase of the luminescence decay time $\tau_{Rx}^{\exp}(T)$ is remarkable. After reaching the maximal value $\tau_{Rx\,\max}^{\exp}\approx 20$ μs at $T=7$ K the radiative lifetime decreases to about 6 μs. Then a fast radiative decay time occurring for $T>50$ K is observed, likely caused by the same thermal quenching process which dominates the steady-state PL.

III. DISCUSSION

As noted above, the short wavelength part of the emission spectra is caused by the recombination of excitons bound to the electron-attractive centers. These centers in $2H$-WS_2 are formed by diatomic halogen molecules unambiguously positioned within the van der Waals gap: Spectra obtained for WS_2 grown with I_2 or Br_2 as transport agents are quite different in their linewidth and peak positions but with a similar temperature behavior strongly implying that the PL is related to the respective molecules; in addition WSe_2 crystals grown with a halogen transport agent display excitonic luminescence while crystals grown without do not.[18] We wish to point out that in the case of $2H$-WS_2, the Br_2 molecule dimensions are very well matched to the host crystalline lattice and are almost ideal for insertion within the interstitial

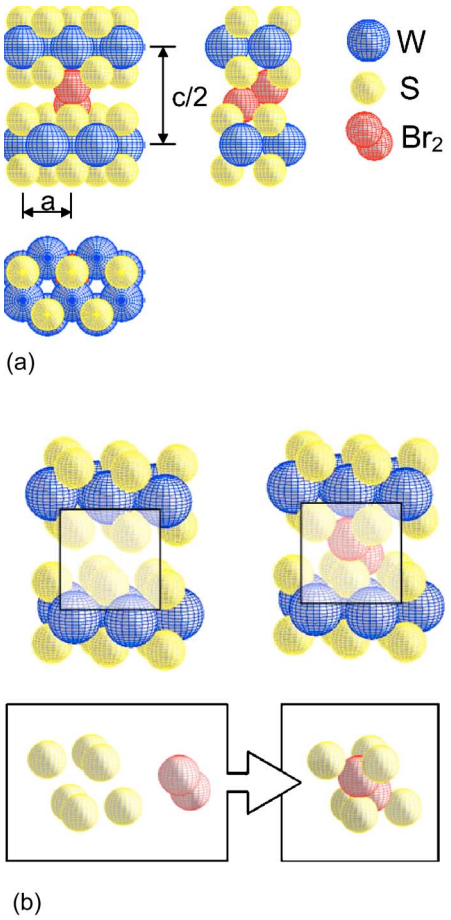

FIG. 5. (Color online) (a) Three projections of the $2H$-WS_2 crystalline lattice fragment with a Br_2 molecule positioned in the van der Waals gap. The large black (blue in color version) spheres represent tungsten (W), the small light grey (yellow), sulfur (S), and the dark grey (red), bromine (Br) atoms. The atomic radius values are represented in the same scale as the lattice parameters and correspond to the atomic radius of the respective elements $r_S=1.035$ Å, $r_W=1.37$ Å, and $r_{Br}=1.145$ Å (see text). (b) Illustration of diatomic halogen molecule intercalation within interstitial quasitetrahedral sites of the $2H$-WS_2 van der Waals gap.

spaces of the two adjacent triangular pyramids (quasitetrahedra) formed by sulphur atoms [Fig. 5(a)]. Indeed, taking into account the $2H$-WS_2 lattice parameters $a=3.153$ Å, $c=12.323$ Å, $z=0.6225$[2] and the S atomic radius $r_S=1.035$ Å, one can show that in each pyramid (quasitetrahedron) a sphere with radius equal to 1.1 Å can be inscribed. This value is very close to the Br atomic radius $r_{Br}=1.145$ Å. The distance between the centers of pyramids with a common lateral side is ~2.3 Å, just equal to $2r_{Br}$—the intramolecular bromine-bromine distance. Owing to this excellent matching, the Br_2 molecules used as a transport agent in the crystal growth process are readily intercalated in well-defined locations within the van der Waals gap [Fig. 5(b)].

In order to explain the behavior of the experimentally measured decay time as a function of temperature $\tau_{Rx}^{meas}(T)$, taking into account the fact that there are at least three zero-phonon lines in the steady-state PL spectra, Eq. (7) as de-

rived by Bergman *et al.*,[29] which describes the decay from any thermalized many-level system, will be used

$$\tau_{Rx}(T) = \frac{\sum_{i=1}^{N} (g_i/g_1)\exp(\Delta_{i1}/kT)}{\sum_{i=1}^{N} [\tau_{Ri}^{-1} + \tau_{th}^{-1}(E_a)](g_i/g_1)\exp(-\Delta_{i1}/kT)}, \quad (1)$$

where Δ_{i1} is the energy between the ith level and the lowest excited level $i=1$ ($\Delta_{11}=0$), g_i is the degeneracy of the ith level and $\tau_{th}(E_a)$ is the decay time of the thermal quenching. It is assumed[29,30] that this quenching is due to a single thermally activated process

$$\tau_{th}^{-1}(E_a) = \tau_0^{-1} \times \exp(-E_a/kT), \quad (2)$$

where E_a is the activation energy and τ_0^{-1} is of the order of the phonon frequency 10^{12}–10^{13} s^{-1}, and does not depend on temperature.

The redistribution of the steady-state PL intensity as the temperature increases in favor of the short wavelength lines B, and then C, is a demonstration that the transition probabilities from the upper excitonic states are higher than from the lower ones (i.e., the respective radiative lifetimes are shorter). In this situation, the relative contributions in the excitonic radiative recombination of the upper levels become dominant as their thermal population increases.[31] However, the rising part of the experimental dependence $\tau_{Rx}^{exp}(T)$ at $T<7$ K, where only the low-energy A line is observed in the steady-state spectrum, means that between the two levels responsible for A and B lines there is an intermediate excited state A^* with a radiative lifetime much longer than the lifetime of the lowest excitonic level—-i.e., the radiative transition from this state is forbidden (Fig. 6). As a result, even though the A^* level is populated already at lowest temperatures, its contribution to the steady-state spectrum is very weak and experimentally it can be revealed only in the luminescence-decay-time temperature dependence. This situation is not typical of other indirect band gap semiconductors that exhibit bound exciton luminescence[19,20,29] where the lowest state is characterized by the longest lifetime value.

The best fit of Eq. (1) to experimental data was obtained with: $\tau_1=10$ μs, $\tau_2 \geqslant 1$ ms, $\tau_3=2.5$ μs, $\tau_4 \cong 0.5$ μs, $\Delta_{21}=0.3$ meV, $E_a=0.1$ eV, $g_1=g_4=1$, $g_2=g_3=2$. Energy values for $\Delta_{31}=\Delta_{AB}=3.0$ meV, and $\Delta_{41}=\Delta_{AC}=13$ meV were taken from the steady state spectra. It should be pointed out that the shape of the calculated $\tau_{Rx}(T)$ is rather insensitive to the lifetime of the second level, as long as τ_2 is greater than 1 ms. The activation energy E_a of the quenching process is practically the same as for steady-state luminescence. The pre-exponential factor τ_0^{-1} was taken equal to the frequency of the most prominent local vibronic mode, $E_{ph2}=30.7$ meV ($\tau_0^{-1}=7.3\times10^{12}$ s^{-1}).

The temperature dependence of the A,B, and C spectral line intensities can be described using an excitonic recombination kinetic model, similar to the model proposed for n-type GaP:N (Ref. 32) (Fig. 7). Because of the small value of the majority-carrier concentration in n-2H-WS_2, the nonradiative excitonic recombination due to Auger processes is considered negligible. Another recombination shunt channel involving the broadband IR emission via T_2-deep level will be described by the hole shunt-path capture time τ_S (see below).

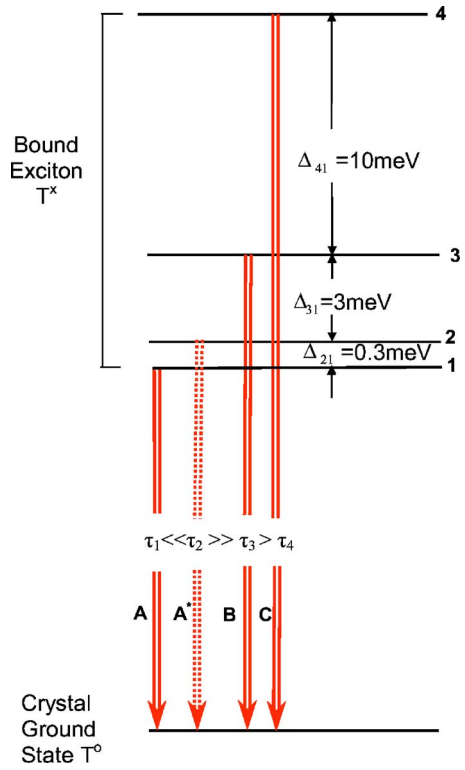

FIG. 6. (Color online) Schematic representation of bound-exciton states and radiative transitions in 2H-WS_2:Br_2 layered crystals. The dashed arrow corresponds to the forbidden radiative transition experimentally revealed from the temperature dependence of the luminescence decay time.

Under the assumptions of low-level excitation and thermal equilibrium the equations, which describe the kinetic behavior of minority carriers in n-type material, are given as follows:[32]

$$\dot{N}_{T1}^{x} = p \times \upsilon_{th} \times \sigma_{px}(N_{T1}^{e} - N_{T1}^{x}) - \frac{N_{T1}^{x}}{\tau_{Rx}} - \frac{N_{T1}^{x}}{\tau_{xp}}, \quad (3a)$$

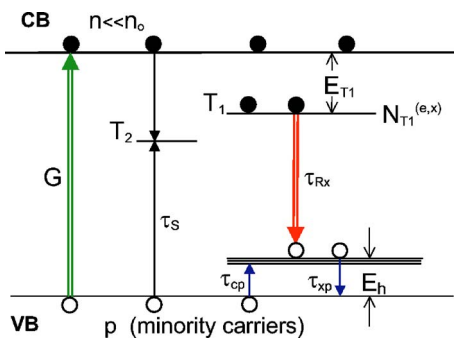

FIG. 7. (Color online) The kinetic model of the recombination emission in 2H-WS_2 containing neutral radiative centers T_1, formed by Br_2 intercalated molecules, and a shunt recombination channel, which includes the deep level T_2, responsible for broadband emission (Ref. 21).

$$\dot{p} = G - p \times \upsilon_{th} \times \sigma_{px}(N^e_{T1} - N^x_{T1}) + \frac{N^x_{T1}}{\tau_{xp}} - \frac{p}{\tau_S}. \quad (3b)$$

Here p is the concentration of the minority holes, N^e_{T1} the concentration of electron-occupied centers, N^x_{T1} the concentration of centers which have an exciton bound to the site, τ_{Rx} is the bound exciton radiative recombination time defined by Eq. (1) without thermal quenching term [i.e., $E_a \to \infty$, $\tau^{-1}_{th}(E_a)=0$], $\tau_{xp}(\tau_{px})$ is the exciton hole capture (thermalization) time, σ_{px} is the hole capture cross section by electron occupied centers, υ_{th} is thermal velocity of minority carriers, and G is the excitation rate.

From the steady-state solution ($\dot{N}^x_{T1}, \dot{p}=0$) of Eqs. (3a) and (3b), assuming that at low-level excitation in n-type material $N^e_{T1} \gg N^x_{T1}$, the following relationship results for the quantum efficiency η_{Rx} of the excitonic radiative recombination:

$$\eta_{Rx} = \frac{N^x_T}{\tau_{Rx}} \times \frac{1}{G} = \left[1 + \frac{\tau_{cp}}{\tau_S}\left(1 + \frac{\tau_{Rx}}{\tau_{xp}} \right) \right]^{-1}, \quad (4)$$

where $\tau_{cp} \equiv (\upsilon_{th} \times \sigma_{px} \times N^e_{T1})^{-1}$ is defined as the capture time of holes by electron-occupied radiative centers. Furthermore, taking into consideration the fact that in thermal equilibrium the bound excitons are canonically distributed amongst the four sublevels, $N^x_{T1} = \Sigma^4_{i=1} N^x_i$, i.e.,

$$N^x_i / g_i = (N^x_j / g_j) \exp(-\Delta_{ji}/kT), \quad (5)$$

the quantum efficiencies of each excitonic line in the steady-state PL spectra defined as

$$\eta_i(T) = \frac{N^x_i(T)}{\tau_i \cdot G}, \quad \eta_{Rx}(T) = \sum_{i=1}^{4} \eta_i(T) \quad (6)$$

may be presented in the following form:

$$\eta^{(A)}_1(T) = \eta_{Rx}(T)\left[1 + \frac{\tau_1}{\tau_2}\frac{g_2}{g_1}\exp\left(\frac{-\Delta_{21}}{kT} \right) + \frac{\tau_1}{\tau_3}\frac{g_3}{g_1}\exp\left(-\frac{\Delta_{31}}{kT} \right) + \frac{\tau_1}{\tau_4}\frac{g_4}{g_1}\exp\left(-\frac{\Delta_{41}}{kT} \right) \right]^{-1}, \quad (7)$$

$$\eta^{(B)}_3(T) = \eta_{Rx}(T)\left[1 + \frac{\tau_3}{\tau_1}\frac{g_1}{g_3}\exp\left(\frac{\Delta_{31}}{kT} \right) + \frac{\tau_3}{\tau_2}\frac{g_2}{g_3}\exp\left(\frac{\Delta_{32}}{kT} \right) + \frac{\tau_3}{\tau_4}\frac{g_4}{g_3}\exp\left(-\frac{\Delta_{43}}{kT} \right) \right]^{-1}, \quad (8)$$

$$\eta^{(C)}_4(T) = \eta_{Rx}(T)\left[1 + \frac{\tau_4}{\tau_1}\frac{g_1}{g_4}\exp\left(\frac{\Delta_{41}}{kT} \right) + \frac{\tau_4}{\tau_2}\frac{g_2}{g_4}\exp\left(\frac{\Delta_{42}}{kT} \right) + \frac{\tau_4}{\tau_3}\frac{g_3}{g_4}\exp\left(\frac{\Delta_{43}}{kT} \right) \right]^{-1}. \quad (9)$$

It should be noted that the contribution of the second excitonic A^* sublevel $\eta^{(A^*)}(T)$, which is unambiguously revealed in the experimental $\tau^{\exp}_{Rx}(T)$ dependence at lowest temperatures, is negligible compared to that of the dominant A line: $\eta^{(A^*)}_2 / \eta^{(A)}_1 \approx \tau_1 / \tau_2 \sim 10^{-3}$. Equations (4) and (7)–(10) describe the temperature behavior of the radiative recombination intensity through the lifetimes $\tau_{Rx}(T), \tau_i, \tau_{cp}(T), \tau_{xp}(T)$, and τ_S.

Before fitting the experimental results shown in Fig. 4, it is necessary to identify the origin of the fast thermal luminescence quenching, which occurs at $T > 50$ K, in order to determine the lifetimes responsible for this process. As was mentioned earlier, the activation energy of the exponential decay coincides with the difference $E^{ind}_g - E_{A,B} \cong 1.45$–$1.32$ eV $= 0.13$ eV. This equality suggests that the abrupt quenching is caused by the thermal depopulation of the electron-attractive centers involved in the radiative recombination (lifetimes τ_{cp} and τ_{xp}), rather than by a nonradiative multiphonon recombination process with the same value of the thermal activation energy.[33]

The capture time of holes $\tau_{cp}(T)$ is governed by the temperature dependence of the concentration of the electron-occupied radiative centers N^e_{T1}, which are in thermal equilibrium with the majority-carrier concentration n_0. At low-level excitation and non-degenerate conditions the occupation probability $f^e_{T1} = N^e_{T1} / N_{T1}$ can be written as[34]

$$f^e_{T1} = \left[1 + g_T \frac{N_C}{n_0} \exp(-E_{T1}/kT) \right]^{-1}, \quad (10)$$

where g_{T1} is the level degeneracy, E_{T1} is the binding energy of the electron on the center, and N_C is the density of states of the conduction band with electron effective mass m_e

$$N_C = 2(2\pi \times m_e \times kT/h^2)^{3/2}. \quad (11)$$

The N_C value, as well as the value of N_V (see below) for WS_2, has been calculated assuming that $m_e = m_h \cong m_0$ (m_0 is the free electron mass), as in the related compounds WSe_2 and $MoSe_2$.[11,35,36]

In the temperature range of the PL quenching ($T = 60$–100 K) the temperature dependence $n_0(T)$ is essentially constant $n_0(T < 120\ \text{K}) \approx 10^{10}\ \text{cm}^{-3}$. Inserting the experimental data on n_0 at low temperature in Eq. (10), the calculated value of N_C, the electron binding energy $E_{T1} \approx 0.1$ eV (taking into account, that $E_{T1} + E_h \cong E_g - E_{A,B}$) and $g_{T1} = 1$, it can be shown that the function f^e_{T1} has a similar temperature behavior as the excitonic luminescence intensity: $f^e_{T1} = 1$ at $T < 50$ K; between 50 and 100 K, when the Fermi level goes down through the T_1 level, $f^e_{T1}(T)$ decreases by five orders of magnitude. This thermalization of the electron-attractive centers leads to the dissociation of the bound excitons. In essence, the PL quenching due to the thermal depopulation of the T_1 center in steady-state conditions is equivalent to the single thermally activated process, described by Eq. (2) for pulsed PL excitation, i.e., $E_{T1} = E_a$.

The excitonic-hole thermalization time depends on the temperature as[37]

$$\tau_{xp} = 2 \times \exp(E_h/kT)(\sigma_{px} \times \nu_{th} \times N_V)^{-1}, \quad (12)$$

where 2 is the spin degeneracy factor, E_h is the hole binding energy, N_V is the density of states in the valence band defined similarly as N_C [Eq. (12)] with the hole effective mass m_h, $\nu_{th} = \sqrt{3 \times kT/m_h}$ is the thermal velocity of the holes.

Using Eqs. (6)–(9), the resulting fit to the experimental data is shown by solid lines in Fig. 3. It should be noted that

above 30 K, the accuracy of the $I_A(T)$ measurements is affected by the overlap with the strong B line. In addition to the parameter values used in the fit of the lifetime temperature dependence, the following parameters are introduced: $E_{T1}=E_a\cong 0.1$ eV, $E_h=0.03$ eV, $\tau_S=2\times 10^{-8}$ s, $N_{T1}\cong 10^{19}$ cm^{-3}, and $\sigma_{px}\cong 10^{-16}$ cm^2.

The evaluation of the binding energies E_{T1} and E_h is based on the analysis of PL exponential thermal decay taking into consideration the free electron density in the samples, and practically does not depend on unknown parameters. The concentration N_{T1} corresponds to the content of bromine in the WS_2 samples measured by x-ray analysis. Finally, the adjusted value of the last parameter σ_{px} is in a good agreement with analogous values for typical isoelectronic centers in GaP.[34,37–39]

The value of the hole shunt-path capture time τ_S is essentially shorter than the measured excitonic radiative time $\tau_{Rx}(T)$. Apparently the recombination channel responsible for IR broadband emission acts as a shunt, which contributes to the thermal quenching of the excitonic emission at $T>60$ K. However, as mentioned above, the integral intensity of this emission does not change (increase) when the much more intense excitonic luminescence quenches (Fig. 1). This indicates that the capture time τ_S is determined mainly by an additional nonradiative recombination process, which is much faster than the radiative one. Both recombination processes are due to deep centers associated, presumably, with intrinsic defects of the WS_2 crystalline lattice.

IV. CONCLUSION

The strong bound exciton luminescence of the 2*H*-WS_2:Br_2 layered compound is due to the neutral centers formed by bromine molecules incorporated in the interstitial sites of the van der Waals gap during the growth of the synthetic crystals. It should be interesting to extend the excitonic PL study to WS_2 thin films[10,11,40] and commercial powders having been submitted to an intercalation process in a bromine atmosphere.

ACKNOWLEDGMENTS

We would like to thank Ernest Arushanov, Christian Kloc, and Boris Tsukerblat for fruitful discussions, and Markus Klenk for x-ray analysis of the samples. We gratefully acknowledge the support in the growth of samples by Hamidreza Riazi-Nejad.

[1] A. Wilson and A. D. Yoffe, Adv. Phys. **18**, 193 (1969).
[2] W. J. Schutte, J. L. de Boer, and F. Jellinek, J. Solid State Chem. **70**, 207 (1987).
[3] R. Coehoorn, C. Haas, J. Dijkstra, C. J. F. Flipse, R. A. de Groot, and A. Wold, Phys. Rev. B **35**, 6195 (1987).
[4] A. Klein, S. Tiefenbacher, V. Eyert, C. Pettenkofer, and W. Jaegermann, Phys. Rev. B **64**, 205416 (2001).
[5] Karsten Albe and Andreas Klein, Phys. Rev. B **66**, 073413 (2002).
[6] C. Sourisseau, F. Cruege, M. Fouassier, and M. Alba, Chem. Phys. **150**, 281 (1991).
[7] K. K. Kam and B. A. Parkinson, J. Phys. Chem. **86**, 463 (1982).
[8] V. Douay and O. Gorochov, J. Chim. Phys. Phys.-Chim. Biol. **83**, 247 (1986).
[9] E. Arushanov, E. Bucher, K. Friemelt, O. Kulikova, L. Kulyuk, A. Nateprov, and A. Siminel, *Proceedings of the 19th International Semicond. Conference CAS-96, Romania* (IEEE, Institute of Microtechnology of Romania, 1996).
[10] C. Ballif, M. Regula, and F. Levy, Sol. Energy Mater. Sol. Cells **57**, 189 (1999).
[11] C. Ballif, M. Regula, P. E. Schmid, M. Remskar, R. Sanjines, and F. Levy, Appl. Phys. A: Mater. Sci. Process. **62**, 543 (1996).
[12] R. H. Friend and A. D. Yoffe, Adv. Phys. **36**, 2 (1987).
[13] S. K. Srivastava and B. N. Avasthi, J. Mater. Sci. **20**, 3801 (1985).
[14] S. H. El-Mahalawy and B. L. Evans, Phys. Status Solidi B **79**, 713 (1977).
[15] W. Y. Lyang, in *Intercalation in Layered Materials*, edited by M. S. Dresselhaus (Plenum Press, New York, 1986), Part. II, p. 31.
[16] Ali Hussain Reshak and S. Auluck, Phys. Rev. B **68**, 125101 (2003).
[17] M. S. Dresselhaus and G. Dresselhaus, Adv. Phys. **30**, 139 (1981); **51**, 1 (2002).
[18] L. Kulyuk, E. Bucher, L. Charron, E. Fortin, A. Nateprov, and O. Schenker, Nonlinear Opt. **29**, 501 (2002).
[19] J. Dean and D. C. Herbert, in *Excitons*, edited by K. Cho (Springer, New York, 1979), p. 55.
[20] J. Weber, W. Schmid, and R. Sauer, Phys. Rev. B **21**, 2401 (1980).
[21] L. Kulyuk, L. Charron, and E. Fortin, Phys. Rev. B **68**, 075314 (2003).
[22] *Photoelectrochemistry and Photovoltaics of Layered Semiconductors*, edited by A. Aruchamy (Kluwer Academic Publishers, Dordrecht, The Netherlands, 1992)
[23] S. V. Prasad and J. S. Zabinski, J. Mater. Sci. Lett. **12**, 1413 (1993).
[24] M. Remskar, A. Mrzel, Z. Skraba, A. Jesih, M. Ceh, J. Demsar, P. Stadelmann, F. Levy, and D. Mihailovic, Science **242**, 479 (2001).
[25] Matthieu Verstraete and Jean-Christophe Charlier, Phys. Rev. B **68**, 045423 (2003).
[26] G. Lucovsky, R. M. White, J. A. Benda, and J. F. Revilli, Phys. Rev. B **7**, 3859 (1973).
[27] A. M. Stacy and D. T. Hodul, J. Phys. Chem. Solids **46**, 405 (1985).
[28] Shin-ichi Uchida and Shoji Tanaka, J. Phys. Soc. Jpn. **45**, 153 (1978).
[29] P. Bergman, B. Monemar, and M. E. Pistol, Phys. Rev. B **40**, 12280 (1989).
[30] M. D. Sturge, E. Cohen, and K. F. Rodgers, Phys. Rev. B **15**, 3169 (1977).
[31] D. G. Thomas, M. Gershenzon, and J. J. Hopfield, Phys. Rev.

131, 2397 (1963);D. G. Thomas and J. J. Hopfield, *ibid.* **150**, 680 (1966); T. N. Morgan, B. Weber, and R. N. Bhargava, *ibid.* **166**, 751 (1968).

[32] P. D. Dapkus, W. H. Hackett, Jr., O. G. Lorimor, and R. Z. Bachrach, J. Appl. Phys. **45**, 4920 (1974).

[33] *Deep Centers in Semiconductors: A State of the Art Approach*, edited by S. T. Panteleides (Gordon and Breach, New York, 1992), p. 591.

[34] J. S. Blakemore, *Semiconductor Statistics* (Pergamon Press, Oxford, 1962)

[35] J. Baglio, E. Kamieniecki, N. DeCola, C. Struck, J. Marzik, K. Dwight, and A. Wold, J. Solid State Chem. **49**, 166 (1983).

[36] Th. Finteis, M. Hengsberger, Th. Straub, K. Fauth, R. Claessen, P. Auer, P. Steiner, S. Hufner, P. Blaha, M. Vogt, M. Lux-Steiner, and E. Bucher, Phys. Rev. B **55**, 10400 (1997).

[37] J. M. Dishman and M. DiDomenico, Jr., Phys. Rev. B **1**, 3381 (1970).

[38] J. S. Jayson and R. Z. Bachrach, Phys. Rev. B **4**, 477 (1971).

[39] M. Sternheim and E. Cohen, Phys. Rev. B **22**, 1875 (1980).

[40] O. Lignier, G. Couturier, and J. Salardenne, Thin Solid Films **338**, 75 (1999).